Nonmagnetic γ''-FeN thin films epitaxially grown on Cu(001): Electronic structure and thermal stability

Cristina Navio,[1,*] Jesus Alvarez,[1] Maria Jose Capitan,[2] Felix Yndurain,[1] and Rodolfo Miranda[3]
[1]*Departamento de Física de la Materia Condensada e Instituto Nicolas Cabrera, Universidad Autónoma de Madrid, Cantoblanco, 28049 Madrid, Spain*
[2]*Instituto de Estructura de la Materia, CSIC, c/Serrano 119, 28006 Madrid, Spain*
[3]*Departamento de Física de la Materia Condensada e Instituto Nicolas Cabrera, Universidad Autónoma de Madrid, Cantoblanco, 28049 Madrid, Spain and Instituto Madrileño de Estudios Avanzados en Nanociencia (IMDEA-Nanociencia), 28049 Madrid, Spain*
(Received 21 May 2008; revised manuscript received 15 September 2008; published 14 October 2008)

We report on a theoretical and experimental study of the growth, electronic structure, and thermal stability of ultrathin films of nonmagnetic iron nitride. The films are grown by evaporation of Fe, in a flux of atomic N produced by a plasma source, onto a Cu(001) surface kept at 300 K and characterized by x-ray photoelectron spectroscopy, ultraviolet photoelectron spectroscopy, and x-ray diffraction. The compound formed is identified as γ''-FeN(001) growing epitaxially on the substrate. Its electronic structure and thermal stability has been studied and compared with first-principles calculations. This nitride film transforms to magnetic γ'-Fe_4N phase by annealing above 650 K, opening new perspectives for applications of these films in functional magnetic nanostructures.

DOI: 10.1103/PhysRevB.78.155417 PACS number(s): 73.20.−r, 71.20.−b, 71.15.Mb, 68.37.Ef

I. INTRODUCTION

Epitaxial films of magnetic iron nitrides[1] are raising renewed interest due to their chemically inert and mechanically hard surfaces, which, together with their intrinsic magnetic properties, makes them suitable as magnetic layers alternative to pure Fe in devices such as reading heads for magnetic storage devices.[2]

The known magnetic iron nitrides are concentrated in the N-poor part of the Fe-N phase diagram. Much interest in α''-$Fe_{16}N_2$ was driven by claims of a magnetic moment of 2.9-Bohr magnetons per Fe atom, larger than in bulk bcc Fe,[3–5] a claim not confirmed later by subsequent experiments due to difficulties in preparing a pure phase or in knowing precisely the amount of active phase present in the samples.[6] Therefore most of the interest in magnetic nitrides moved to γ'-Fe_4N, which, on the contrary, is a compound with well-defined crystalline structure and magnetic properties. This cubic phase is ferromagnetic at a Curie temperature of 767 K and a saturation magnetization of 1.8 T. It can be grown epitaxially over a variety of substrates.[7–10]

In the N-rich part of the Fe-N phase diagram, other weakly magnetic or nonmagnetic iron nitrides have been found.[11] Increasing the amount of N quickly decreases the magnetic moment as the cubic iron sublattice transforms into the ε hexagonal phase that can accept from 25 at. % to 33 at. % of N atoms randomly distributed in the octahedral sites of the Fe sublattice.[6] At the Fe_2N stoichiometry, the ε phase can result in ζ-Fe_2N, which has an orthorhombic structure, by ordering the N atoms over the octahedral sites. This phase is possibly a weak itinerant ferromagnet at very low temperature,[12] but it is not magnetic above 9 K.

At even higher concentrations of N, there have been reports of the existence of two compounds with an FeN stoichiometry: nonmagnetic γ''-FeN, with the zinc-blende (ZS) structure, and γ'''-FeN, with the NaCl crystalline structure and probably antiferromagnetic.[12,13] Almost nothing is known concerning the electronic structure and properties of these compounds.

Here we report on the growth, chemical composition, crystallography, and electronic structure (chemical bonding, core and valence band states, and density of states), as determined by both experimental and theoretical techniques, of iron nitride films grown onto a Cu(001) surface at 300 K. Under our experimental conditions, the phase which is stable at 300 K is nonmagnetic, zinc-blende γ''-FeN. In analogous experimental conditions, but keeping the substrate at 700 K during the film growth, magnetic γ'-Fe_4N(001) films is formed.[7,9] We also show that annealing above 650 K causes the FeN film to decompose into stable, magnetic γ'-Fe_4N(001). This behavior could be potentially useful in writing magnetic dots on a nonmagnetic matrix.[14] Such dots could be coupled through a Cu spacer layer with a magnetic underlayer.

II. EXPERIMENTAL AND THEORETICAL METHODS

The experiments were performed in an ion-pumped ultrahigh vacuum (UHV) chamber with a base pressure on the order of 10^{-10} mbar, equipped with an x-ray source (Mg K_α, photon energy of 1253.6 eV), a discharge lamp to provide photons with energies of 21.22 eV (He-I) and 40.8 eV (He-II), electron and ion guns, and a low-energy electron diffraction (LEED) apparatus. These sources allowed us to perform x-ray photoelectron spectroscopy (XPS), ultraviolet photoelectron spectroscopy (UPS), and auger electron spectroscopy (AES) using a Leybold-Heraeus Hemispherical Analyzer (LHS10) to detect the ejected electrons or ions. The spectrometer was calibrated with clean single crystal samples to give the Cu $2p_{3/2}$ core level peak at 932.3 eV and the Fe $2p_{3/2}$ peak at 706.7 eV.

Structural characterization was performed by means of *ex situ* x-ray diffraction (XRD) using a six-circle diffractometer with optimized geometry for surface analysis at the W1.1

beamline of the Hasylab synchrotron at DESY with a wavelength of 1.393 Å. The angle of incidence of the x-ray beam was fixed at 2° with respect to the substrate surface.

The substrates used for growing iron nitride films at 300 K were either Cu(001) single-crystals, cleaned *in situ* by cycles of Ar^+ sputtering (1 keV) and annealed at 900 K until no contamination was present in the XPS spectrum, or thin Cu(001) films grown, in turn, on a γ'-Fe_4N film deposited on MgO(001). This late sample was employed for *ex situ* crystallographic measurements. An Fe(001) crystal, used for comparison purposes, was also cleaned inside the UHV chamber by repeated cycles of Ar^+ bombardment (1 keV) and annealing up to 920 K.

The nitride films were grown by depositing Fe from a home-made evaporator at a rate of 0.2 ML/min, while simultaneously exposing the substrate to a flux of atomic nitrogen obtained from a radio-frequency (RF) plasma discharge source.[15] The RF source employed a 1:1 mixture of nitrogen and hydrogen with an internal pressure of 10^{-2} mbar.

The experimental results were compared with first-principles theoretical calculations performed in the context of density functional theory[16] using the SIESTA (Ref. 17) method. For the exchange correlation potential we adopted a generalized gradient approximation.[18] The norm-conserving pseudopotentials used follow the Troullier-Martins scheme[19] in the nonlocal form proposed by Kleinman and Bylander[20] and with partial core corrections.

III. RESULTS AND DISCUSSION

A. Growth of γ''-FeN at 300 K

The iron nitride phase diagram has been extensively studied in the intermediate and high-temperature and iron-rich regions.[11,21,22] It has been well established that γ'-Fe_4N films can be grown epitaxially over different substrates [MgO(001),[7] Cu(001),[7,8] and Fe(001) (Ref. 9)] by evaporating Fe under a flux of nitrogen atoms at 700 K. We shall show now that under the same experimental conditions, but keeping the Cu(001) substrate at room temperature, the resulting iron nitride film corresponds to the γ''-FeN phase.

Figure 1 shows schematically the structure of the samples studied by means of XRD: two different iron nitride layers, separated by a Cu film, were sequentially deposited on MgO(001) substrates. The lower (γ'-Fe_4N) layer was grown at 700 K and used as a reference, whereas the upper iron nitride layer was grown at room temperature. MgO(001) was chosen as a substrate because it is known that γ'-Fe_4N grows epitaxially on it,[7,9] and its characteristic Bragg peaks are far from the region of the reciprocal space of interest for characterizing the different iron nitrides.

Figure 2 shows the radial integrated intensity along the (111) direction for one of these samples. The inset shows the measured two-dimensional (2D) x-ray diffraction diagram, where the Bragg peaks contain both perpendicular and parallel momentum transfer, thus giving information on both in-plane and out-of-plane structures. The ordinate units in the inset are related to the substrate reciprocal lattice units (r.l.u.), i.e., the MgO (111) intense Bragg peak appears at r.l.u. equal to 1, whereas the peak that appears at 1.167 r.l.u.

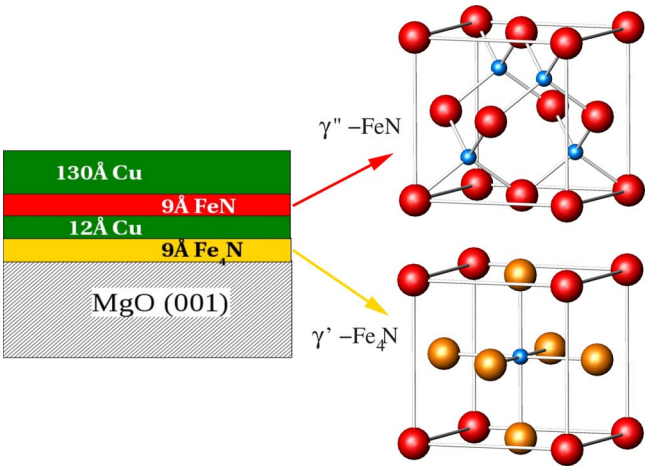

FIG. 1. (Color online) Schematic representation of the samples grown for *ex situ* measurements and the crystalline structure of relevant iron nitrides. On a MgO(001) substrate, a film of γ'-Fe_4N was first deposited at 700 K. A Cu(001) layer was then deposited to act as a substrate for the subsequent deposition of γ''-FeN at 300 K. The sample was finally covered with a protective Cu layer for *ex situ* measurements.

corresponds to the Cu(111) Bragg peak from the copper layers. In addition, two other peaks appear in the x-ray pattern, reflecting the two different iron nitride structures. The peak at r.l.u.=1.111 corresponds to a lattice parameter of 3.795 Å, i.e., the (111) interlayer distance of γ'-Fe_4N. The in-plane dispersion for this phase is almost the same as the one corresponding to the MgO substrate, indicating the high in-plane epitaxy of the γ'-Fe_4N with respect to the substrate. The peak at 0.979 r.l.u. corresponds to a lattice parameter of 4.307 Å, i.e., that of γ''-FeN with the fcc zinc-blende-type structure shown in Fig. 1. In this case, the radial scan indi-

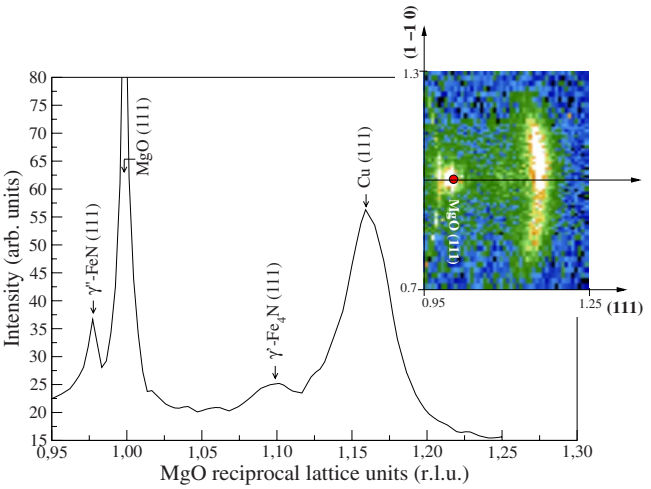

FIG. 2. (Color online) 2D x-ray diffraction diagram in the $[\bar{1}\bar{1}2]$ plane and along the (111) axis for a sample composed of two iron nitride layers separated by Cu, grown on MgO(001). The lower iron nitride layer, deposited at 700 K, has a cubic γ'-Fe_4N structure and was epitaxially grown with a (001) orientation with respect to the substrate. The iron nitride layer deposited at 300 K has a γ''-FeN structure with a (001) orientation.

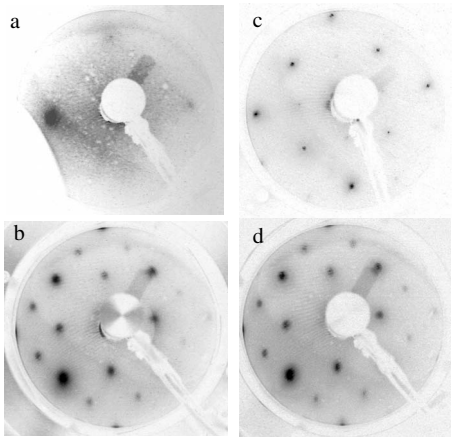

FIG. 3. LEED pattern for (a) a 32-Å-thick iron nitride film grown at 300 K on Cu(001), to be compared with: (c) a $c(2\times2)$ superstructure of N adsorbed on Fe(001) and (d) a γ'-$Fe_4N(001)$ thin film with its $pg4m$ surface reconstruction, used as references. LEED pattern (b) corresponds to the iron nitride film depicted in (a) after annealing a 715 K for 10 min. The LEED patterns were recorded at 60 eV, except for (a), which was taken at 23.4 eV and exhibits some distortions.

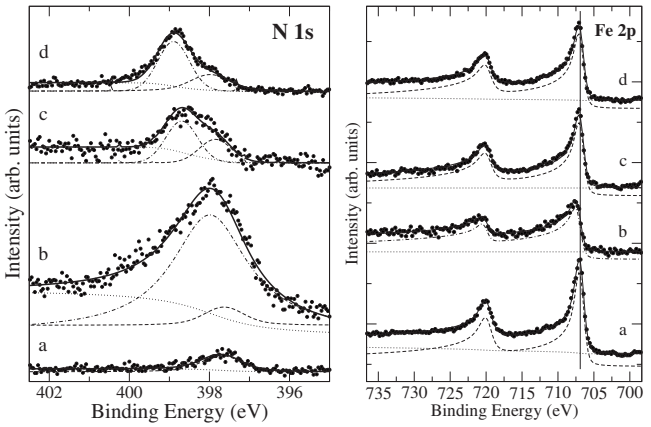

FIG. 4. XPS core levels of N 1s (left panel) and Fe 2p (right panel) for: (a) a Fe(001) crystal with a half surface monolayer of N forming in a $c(2\times2)$ superstructure; (b) a 32-Å-thick iron nitride film grown at 300 K on Cu(001); (c) the same iron nitride film after annealing at 715 K for 10 min; and (d) a reference γ'-$Fe_4N(001)$ thin film.

cates that these crystals have a large mosaic block size, but its angular dispersion is quite large compared to the MgO or γ'-Fe_4N (see the 2D diagram in the inset of Fig. 2). This dispersion is reproduced in the Cu capping layer, as indicated by the corresponding peak width in the inset of Fig. 2.

In order to characterize in detail the thermal stability of γ''-FeN, thin films were also grown under UHV conditions directly on Cu(001) substrates at 300 K. Figure 3(a) shows the LEED pattern obtained *in situ* for a 32-Å-thick- (as given by small-angle x-ray reflectivity) iron nitride film grown on Cu (001). The pattern is consistent with an unreconstructed γ''-FeN(001) structure with a reduced degree of long-range order, confirming that the γ''-FeN thin film grown at 300 K is epitaxial with the Cu(001) substrate and presents the (001) orientation. As a reference, Fig. 3(c) shows the pattern for a $c(2\times2)$ superstructure of N adsorbed on Fe(001). Figure 3(d) shows the LEED pattern of γ'-$Fe_4N(001)$, with its characteristic $pg4m$ surface reconstruction,[8] whereas Fig. 3(b) reproduces the LEED pattern of the 32-Å-thick iron nitride film grown at 300 K on Cu (001) and heated to 715 K. Notice the evident similarity of the patterns in (b) and (d), which will be discussed below.

The identification of the iron nitride film grown at 300 K as γ''-FeN is confirmed by XPS. Since all the Fe and N atoms in films of the explored thicknesses are within the escape-depth of photoelectrons excited by incident x-rays, the ratio of the Fe $2p_{3/2}$ and N 1s peak areas (see Fig. 4 below)[23] can be used to determine the average chemical composition of the films following standard procedures[24] by using the atomic sensitivities determined previously for this particular spectrometer.[9,25] The resulting ratio is $Fe_{1.1\pm0.2}N$. This composition is clearly different from the one ($Fe_{4.0\pm0.2}N$) obtained under the same experimental conditions, but keeping the Cu(001) substrate at 700 K.[9]

We can conclude that the iron nitride compound grown at 300 K has a γ''-FeN structure epitaxial with the Cu(001) substrate with a limited in-plane dispersion with respect to the Cu atomic axis. Tessier *et al.*[26] determined the enthalpy of formation of different iron nitrides at 300 K, finding that γ''-FeN is more stable than γ'-Fe_4N (ΔH_f° are -47.08 ± 3.47 kJ mol^{-1} and -12.17 ± 20.26 kJ mol^{-1}, respectively). Although other authors[21] have proposed that the stable phase at 300 K is α''-$Fe_{16}N_2$, Tessier *et al.* did not consider this phase to be an equilibrium iron nitride, but rather a metastable one (the enthalpy of formation for this phase is 85.2 ± 46.8 kJ mol^{-1}). Our observations agree with their interpretation.

The FeN fcc phase can appear in two possible crystalline structures: a ZB type (γ''-FeN) and a sodium chloride type (γ'''-FeN).[12,27,28] However, the actual existence of both phases for films is still a matter of controversy. Theoretical calculations carried out for both compounds indicate that the sodium chloride phase is not stable.[29,30] Suzuki *et al.*[31] showed that a pure fcc ZB structure with a 1:1 Fe:N composition can be formed by dc reactive sputtering of N_2 at low temperature. We confirm here these results concerning the stability of (γ''-FeN).

B. Electronic structure of γ''-FeN

The iron nitride film grown at 300 K on Cu(001) (film thickness=32 Å as measured by small-angle x-ray reflectivity; data not shown) presents different electronic properties from those of γ'-Fe_4N grown at 700 K. Lukasev and Lambrecht[29] postulated that the ZB structure of this transition-metal nitride might make it an attractive Schottky barrier or Ohmic contact material for semiconductors because it may allow for epitaxial growth with high-quality sharp interfaces. However, there are few experimental studies of its electronic properties. Thus, here we present an exhaustive study of the electronic properties of γ''-FeN.

The iron nitride film grown at 300 K on Cu(001) presents a different degree of charge transfer between Fe and N than γ'-Fe_4N. Figure 4 shows N 1s core level spectra for different

iron nitride films grown on Cu(001). Figure 4(a) shows the N 1*s* spectrum corresponding to a half monolayer of adsorbed N on Fe(001), where all the N is located at the external surface forming a $c(2\times2)$ superstructure. The fit in Fig. 4(a) shows that the main N 1*s* peak in this case is at a binding energy (BE) of 397.6 eV.[9] Figure 4(b) shows the N 1*s* core level for the iron nitride film prepared at 300 K, whose main peak appears at 397.9 eV, 1 eV lower than the BE of bulk γ'-Fe_4N [Fig. 4(d)] but close to the surface N BE. The N at the surface can also be detected clearly as a lower BE peak at 397.7 eV for γ'-Fe_4N. This surface nitrogen XPS position has already been discussed elsewhere.[9,32] Taking into account that the N atoms in the γ''-FeN structure are in tetrahedral sites with four Fe atoms in their nearest-neighbor shell and are out of the Fe atomic plane, it is understandable that the N 1*s* XPS peak appears closer to that of N adsorbed at the Fe(001) surface (where there are also four Fe atoms in the nearest-neighbor shell and the N is slightly out of the Fe plane) than to the γ'-Fe_4N, where the N atoms have a coordination shell of six Fe atoms and are located within the Fe plane.

Right panel of Fig. 4 shows that the Fe $2p_{3/2}$ and $2p_{1/2}$ peaks of the film prepared at 300 K display a noticeable increase in their apparent asymmetry. Its main component is shifted up 0.4–0.5 eV with respect to that of γ'-Fe_4N shown in Fig. 4(d). Increasing the N content in the nitride, then, shifts the N core level to *lower BE* and the Fe core level to *higher BE*, probably as a result of the increasing amount of charge transfer from Fe to N. Our first-principles calculations carried out for ZB fcc γ''-FeN show that Fe has a charge transfer of 0.4 electrons in this iron nitride. This can be compared to similar calculations for γ'-Fe_4N,[9] where two different types of Fe atoms exist (see Fig. 1), one noncoordinated to N atoms (with a charge transfer of 0.1 electrons) and another one coordinated to N (with a charge transfer of 0.3 electron).

For deposition at 300 K, there is no sign of reaction of Fe with the Cu substrate in either the Cu 2*p* core level or in the Cu x-ray-induced, high-energy, LVV AES spectrum (not shown). The lack of oxygen signal in XPS also allows us to rule out the presence of iron oxide compounds.

Figure 5(b) (left panel) shows the UPS spectrum of the as-grown $Fe_{1.1\pm0.2}N$ film. The film is metallic, although with a strongly reduced emission at the Fermi level. The spectrum is very broad and dominated by features of very low intensity at −5 and −7 eV, which correspond to N 2*p* states. The spectrum is similar to one previously reported for an 8 ML, fcc film of Fe/Cu(001) exposed to N_2 at 75 K.[33]

For a complete analysis of the electronic structure of the γ''-FeN films, we have performed a first-principles calculation using the SIESTA code.[17] For the fcc ZB γ''-FeN structure we obtained an equilibrium lattice constant of 4.30 Å, which is almost equal to the experimental one (4.307 Å). Figure 6 shows the calculated bulk band structure for the experimental lattice constant. There are bands crossing the Fermi level, thus giving a metal with a low density of states close to the Fermi level. The calculated bands agree with previous results obtained using a different method of calculation.[29,30]

The calculation of the variation in the total energy of the γ''-FeN phase versus the total magnetic moment of the system (Fig. 6, right panel) clearly shows a nonferromagnetic behavior in agreement with other previous results.[29] *Ex situ* Kerr magnetization measurements of γ''-FeN films grown on Cu (001) confirms the nonferromagnetic character of the structure. Furthermore, the fcc arrangement of the iron atoms in the zinc-blende structure makes it incompatible with a noncomplex antiferromagnetic arrangement due to the geometry related magnetic frustration.

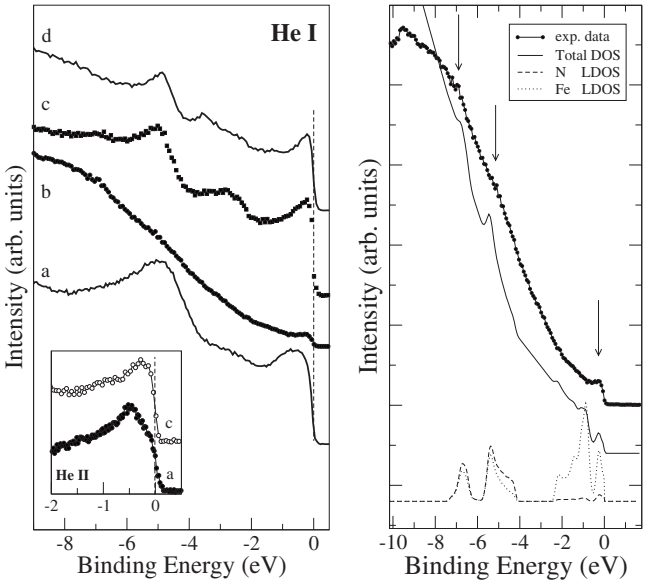

FIG. 5. Left panel: ultraviolet photoelectron spectra recorded using 21.2-eV photons for: (a) a Fe(001) crystal with a half surface monolayer of N forming a $c(2\times2)$ superstructure; (b) a 32-Å-thick iron nitride film grown at 300 K on Cu(001); (c) the same iron nitride film after annealing a 715 K for 10 min; and (d) a reference γ'-Fe_4N(001) film. The inset shows the UPS spectra close to the Fermi level recorded with 40.8-eV photons for samples (a) and (c). In the right panel the dotted lines show the atom-resolved (N and Fe) local density of states calculated for bulk γ''-FeN. The upper curve shows the measured UPS spectrum of γ''-FeN with arrows pointing to the main features. The thin continuous line shows the expected shape of the UPS spectrum taking into account the LDOS for bulk γ''-FeN, the photoionization cross section of Fe and N, their partial density of states, and the integral background of secondary electrons (Ref. 34).

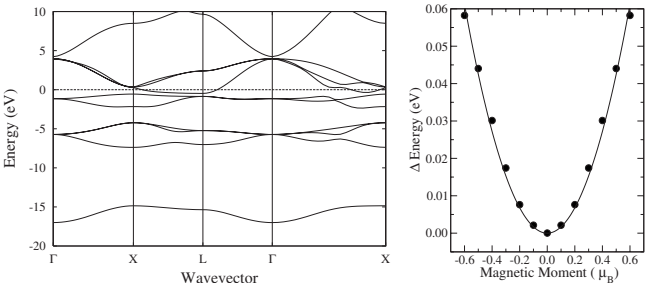

FIG. 6. Left panel: Calculated band structure for bulk paramagnetic γ''-FeN with the zinc-blende structure along the main symmetry directions. The zero of energy is set at the Fermi level. Right panel: calculated total energy variation of the FeN in the zinc-blende structure versus total magnetic moment.

The atom-resolved local density of states (LDOS) calculated for a bulk γ''-FeN is shown in right panel of Fig. 5. The measured UPS spectrum of the as-grown ZB-type iron nitride film is compared with the calculated total LDOS for the bulk considering their partial density of states, the photoionization cross sections of Fe and N, and the integral background of secondary electrons corrected by the electron scattering function.[34] Although the measured UPS spectrum does not show sharp peaks, the broad and low-intensity peaks that appear at −5 and −7 eV are well reproduced. The large background intensity in the spectrum highlights the importance of inelastic collisions of photoemitted electrons on the way out toward the surface.

C. Thermal evolution of the γ''-FeN film

It has been shown that under the present deposition conditions, the iron nitride film grown at 300 K on Cu(001) has an epitaxial γ''-FeN structure. This ZB-type fcc structure is not magnetic. However, it is well known that for the same experimental conditions, but keeping the substrate at 700 K, the resulting film has a γ'-Fe_4N structure, which is magnetic. Thus, we have followed the thermal evolution of the room-temperature phase in order to detect the appearance of γ'-Fe_4N upon thermal annealing.

Figure 3(b) shows the LEED pattern for a γ''-FeN thin film after annealing at 715 K for 10 min. It indicates that the as-grown film has transformed into the γ'-Fe_4N phase [see the corresponding LEED pattern in Fig. 3(d)]. The change in the LEED pattern is observed above 650 K. No change in the Cu LVV spectra (not shown) was detected during the transformation, indicating that there is no diffusion into the Cu substrate of the N atoms released and formation of copper nitrides.[32]

The transformation of γ''-FeN into γ'-Fe_4N upon heating is clearly observed in the photoemission spectra. Figure 4(c) shows the N 1*s* and Fe 2*p* core levels for a γ''-FeN thin film grown at 300 K and annealed *in situ* to 715 K. The relative intensity of the N 1*s* core level decreases, indicating the desorption of N upon annealing. The energy position and the line shape after heating are similar to the spectrum of γ'-Fe_4N shown in Fig. 4(d). The Fe 2*p* core level of the annealed film is strikingly similar to the one of γ'-Fe_4N shown in Fig. 4(d). In fact, all the Fe 2*p* spectra recorded at different temperatures during the annealing process can be fitted with two components corresponding to spectra *b* and *d* of right panel of Fig. 4.[23] The results of the fit are shown in the left panel of Fig. 7. The Fe 2*p* core level corresponds to Fe_4N around 650 K. Additionally, at this temperature, N desorbs from the film and the N 1*s* peak shifts 0.7 eV to higher binding energy as shown in the lower-right panel of Fig. 7.

The structural evolution of the γ''-FeN thin film with annealing temperature can also be detected in the UPS spectra taken with He-I and He-II radiation (see left panel in Fig. 5). The annealed film does not simply contain metallic Fe with adsorbed N. The UPS spectrum corresponding to the $c(2\times2)$ superstructure of N on Fe(001) displays large changes in the vicinity of the Fermi level when changing the photon energy, which can be easily used as a fingerprint. The inset

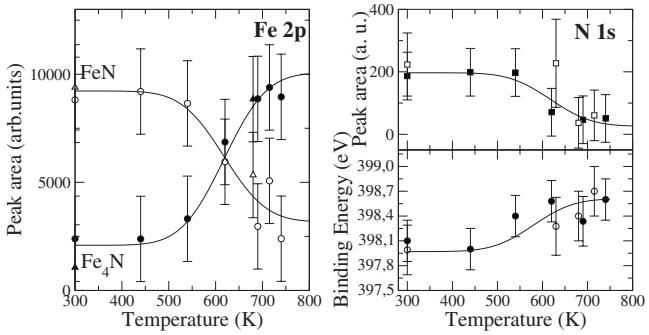

FIG. 7. Left panel: evolution of the different components of the Fe $2p_{3/2}$ core level for a γ''-FeN thin film as a function of temperature. Every experimental spectrum has been fitted with two components, characteristic of FeN, and Fe_4N, respectively, with fixed energy position and peak asymmetry. The panels at the right reproduce the evolution of the N 1*s* integrated intensity (top) and N 1*s* energy position (bottom) as a function of temperature.

(a) in Fig. 5 illustrates this with the spectrum recorded with photons of 40.8 eV, which has a lower density of states close to the Fermi level and a peaklike feature around 0.5 eV below the Fermi level. The same spectrum taken with 21.2-eV photons [see Fig. 5(a)] shows a different shape close to the Fermi level and a rather broad feature centered now around 0.8 eV below Fermi level. These differences can be understood in terms of the band structure of Fe(100). When electrons located in energy close to the Fermi level adsorb a photon of energy 21.2 eV and are emitted perpendicularly to the surface, they have (after subtraction of the crystal inner potential) a crystal momentum in the Γ-H direction close to the H point of the first Brillouin zone. On the contrary, electrons close to the Fermi level, but with a larger kinetic energy provided by He-II photons, have a crystal momentum that corresponds to a point along the Γ-H direction of the second Brillouin zone. The UPS spectrum for annealed FeN film also shown in the inset in the left panel of Fig. 5 is clearly different from the one of $c(2\times2)$N/Fe(100) and confirms that the annealed FeN film does not contain metallic Fe(100) crystallites with adsorbed N, but it has decomposed into γ'-Fe_4N. In fact, the UPS spectrum of annealed FeN [Fig. 5(c)] is identical to the one of γ'-Fe_4N(001) reproduced in Fig. 5(d).

The results described above demonstrate that γ''-FeN transforms into γ'-Fe_4N above 650 K. This explains the observation by Suzuki *et al.*[31] of the appearance of magnetism in single phases of γ''-FeN grown by dc reactive sputtering when heated above 635 K.

IV. CONCLUSIONS

In conclusion, we have grown (001)-oriented thin films of γ''-FeN on Cu(001) and characterized their crystalline structure, chemical composition, and electronic structure comparing with first-principles calculations. Annealing this nonmagnetic film above 650 K transforms it into magnetic, (001)-oriented γ'-Fe_4N. Thus, magnetic properties can be induced

by local annealing of γ'-FeN thin films, which opens possibilities for technological applications in the fabrication of magnetic dots based on the local, thermally induced, controlled transformation of iron nitride thin films from a nonmagnetic to a magnetic state This behavior could be potentially useful in writing magnetic dots or lateral spin valves on a nonmagnetic matrix.[14,35,36] The magnetic dots could be coupled through a Cu spacer layer with a magnetic underlayer.

ACKNOWLEDGMENTS

This work was supported by the Spanish CICyT (under Grants No. FIS 2007-61114, No. MAT2004-05865, No. NAN2004-08881-C02-01, and CONSOLIDER on Molecular Nanoscience), the Comunidad de Madrid (under Grant No. S-0505/MAT-0194), and the EU (under the PF6 "Structuring the European Research Area" program Contract No. RII3-CT-2004-506008).

*cristina.navio@uam.es

[1] J. M. D. Coey and P. A. I. Smith, J. Magn. Magn. Mater. **200**, 405 (1999).
[2] O. Kohmoto, IEEE Trans. Magn. **27**, 3640 (1991).
[3] T. K. Kim and M. Takahashi, Appl. Phys. Lett. **20**, 492 (1972).
[4] Y. Sugita, K. Mitsuoka, M. Komuro, H. Hoshiya, Y. Kozono, and M. Hanazono, J. Appl. Phys. **70**, 5977 (1991).
[5] C. Ortiz, G. Dumpich, and A. H. Morrish, Appl. Phys. Lett. **65**, 2737 (1994).
[6] N. Takahashi, Y. Toda, T. Nakamura, and T. Fujii, Jpn. J. Appl. Phys., Part 1 **38**, 6031 (1999).
[7] J. M. Gallego, S. Y. Grachev, D. M. Borsa, D. O. Boerma, D. Ecija, and R. Miranda, Phys. Rev. B **70**, 115417 (2004).
[8] J. M. Gallego, D. O. Boerma, R. Miranda, and F. Yndurain, Phys. Rev. Lett. **95**, 136102 (2005).
[9] C. Navio, J. Alvarez, M. J. Capitan, D. Ecija, J. M. Gallego, F. Yndurain, and R. Miranda, Phys. Rev. B **75**, 125422 (2007).
[10] D. Ecija, J. M. Gallego, J. Camarero, and R. Miranda, J. Magn. Magn. Mater. **316**, 321 (2007).
[11] B. J. Kooi, M. A. J. Somers, and E. J. Mittemeijer, Metall. Mater. Trans. A **27**, 1063 (1996).
[12] T. Hinomura and S. Nasu, Hyperfine Interact. **111**, 221 (1998).
[13] A. Filippetti and W. E. Pickett, Phys. Rev. B **59**, 8397 (1999).
[14] N. Mohapatra, K. K. Iyer, S. Rayaprol, and E. V. Sampathkumaran, Phys. Rev. B **75**, 214422 (2007).
[15] S. Yu. Grachev, D. M. Borsa, and D. O. Boerma, Surf. Sci. **516**, 159 (2002).
[16] W. Kohn and L. J. Sham, Phys. Rev. **140**, A1133 (1965).
[17] J. M. Soler, E. Artacho, J. D. Gale, A. Garcia, J. Junquera, P. Ordejon, and D. Sanchez-Portal, J. Phys.: Condens. Matter **14**, 2745 (2002).
[18] J. P. Perdew, K. Burke, and M. Ernzerhof, Phys. Rev. Lett. **77**, 3865 (1996).
[19] N. Troullier and J. L. Martins, Phys. Rev. B **43**, 1993 (1991).
[20] L. Kleinman and D. M. Bylander, Phys. Rev. Lett. **48**, 1425 (1982).
[21] E. H. du Marchie van Voorthuysen, N. G. Chechenin, and D. O. Boerma, Metall. Mater. Trans. A **33**, 2593 (2002).
[22] H. A. Wriedt, N. A. Gokcen, and R. H. Nafzinger, in *Phase Diagrams of Binary Iron Alloys*, edited by H. Okamoto (ASM International, Materials Park, OH, 1993), pp. 222–242.
[23] The peaks were fitted, after subtraction of a Shirley background, with an asymmetric Doniach-Sunjic combination of Lorentzian and Gaussian line shapes.
[24] M. P. Seah and W. A. Dench, Surf. Interface Anal. **1**, 2 (1979).
[25] J. Alvarez, J. J. Hinarejos, E. G. Michel, J. M. Gallego, A. L. Vazquez de Parga, J. de la Figuera, C. Ocal, and R. Miranda, Appl. Phys. Lett. **59**, 99 (1991).
[26] F. Tessier, A. Navrotsky, R. Niewa, A. Leineweber, H. Jacobs, S. Kikkawa, M. Takahashi, F. Kanamaru, and F. J. DiSalvo, Solid State Sci. **2**, 457 (2000).
[27] M. Gupta, A. Gupta, P. Bhattacharya, P. Misra and L. M. Kukraja, J. Alloys Compd. **326**, 265 (2001).
[28] L. Rissanen, P. Shaaf, N. Neubauer, K. P. Lieb, J. Keinonen, and T. Sajavaara, Appl. Surf. Sci. **138-139**, 261 (1999).
[29] P. Lukashev and W. R. L. Lambrecht, Phys. Rev. B **70**, 245205 (2004).
[30] Y. Kong, J. Phys.: Condens. Matter **12**, 4161 (2000).
[31] K. Suzuki, H. Morita, T. Kanedo, H. Yoshida and H. Fujimori, J. Alloys Compd. **201**, 11 (1993).
[32] C. Navio, M. J. Capitan, J. Alvarez, F. Yndurain, and R. Miranda, Phys. Rev. B **76**, 085105 (2007).
[33] M. Grune, J. Radnik, and K. Wandelt, Surf. Sci. **402-404**, 236 (1998).
[34] X. Li, Z. Zhang, and V. E. Henrich, J. Electron Spectrosc. Relat. Phenom. **63**, 253 (1993).
[35] M. Johnson, IEEE Trans. Electron Devices **54**, 1024 (2007).
[36] F. J. Jedema, M. S. Nijboer, A. T. Filip, and B. J. van Wees, Phys. Rev. B **67**, 085319 (2003).